Cellular and Molecular Biology
E-ISSN : 1165-158X / P-ISSN : 0145-5680
www.cellmolbiol.org

Effects of Vinblastine and Vincristine on the function of chronic myeloid leukemic cells through expression of A20 and CYLD

Nguyen Huy Hoang[1,2], Nguyen Thanh Huyen[3], Do Thi Trang[1], Nguyen Xuan Canh[3], Can Van Mao[4], Mentor Sopjani[5], Nguyen Ba Vuong[6], Nguyen Thi Xuan[1,2*]

[1] Institute of Genome Research, Vietnam Academy of Science and Technology, 18 Hoang Quoc Viet, Cau Giay, Hanoi, Vietnam
[2] Graduate University of Science and Technology, Vietnam Academy of Science and Technology, 18 Hoang Quoc Viet, Cau Giay, Hanoi, Vietnam
[3] Faculty of Biotechnology, Vietnam National University of Agriculture, Hanoi, Vietnam
[4] Department of Pathophysiology, Vietnam Military Medical University, Ha Dong, Hanoi, Vietnam
[5] Faculty of Medicine, University of Prishtina, Prishtinë, Kosova
[6] 103 Hospital, Vietnam Military Medical University, Ha Dong, Hanoi, Vietnam

ARTICLE INFO

Original paper

Article history:
Received: July 20, 2022
Accepted: August 25, 2022
Published: September 30, 2022

Keywords:

A20, cell death, chronic myelogenous leukemia, CYLD

ABSTRACT

Chronic myelogenous leukemia (CML) is characterised by the translocation of regions of the BCR and ABL genes, leading to the fusion gene BCR-ABL forming the Philadelphia (Ph) chromosome. Vinblastine (Vinb) and Vincristine (Vinc) are Vinca alkaloids and frequently used in combination chemotherapy in leukemias and lymphomas. Deubiquitinating enzyme (DUB) genes such as *A20, Otubain 1* and *CYLD* are known as inhibitors of functional activation of immune cells mediated through the NF-κB/STAT pathway. Little is known about the regulatory role of Vinb/Vinc on the function of CML cells and the contribution of the DUBs to those effects. In the end, the gene expression profile was determined by quantitative RT-PCR, physiological properties of CML cells by flow cytometry and cytokine production by ELISA. As a result, inactivated expression of the DUBs *A20, CYLD, Otubain 1* and *Cezanne* and enhanced activation of $CD11b^+$ and CD4T cells were observed in CML patients. Importantly, Vinc enhanced the expression of *A20* and *CYLD* and inhibited the proliferation and survival of CML (K562) cells. The effects were abolished in the presence of *A20* siRNA, while cell proliferation only depended on the presence of *CYLD*. In conclusion, the up-regulation of *A20* by Vinc could involve inhibitory effects on the proliferation and survival of K562 cells. The events might contribute to the anticancer effect of Vinc on *A20*-sensitive CML cells.

Doi: http://dx.doi.org/10.14715/cmb/2022.68.10.7

Introduction

Chronic myelogenous leukemia (CML) is a myeloproliferative disorder characterized by the uncontrolled growth of myeloid lineage cells in both bone marrow and peripheral blood. The disease is mostly caused by the translocation of regions of BCR and ABL genes, leading to the fusion gene BCR-ABL, which forms the Philadelphia (Ph) chromosome (1). Overexpression of BCR-ABL fusion protein leads to aberrant activation of Janus kinase (JAK)/signal transducer and activator of transcription (STAT) signaling pathway, resulting in uncontrolled proliferation and resistance to apoptosis of CML cells (2). In most cases, CML dramatically improved survival rate after the advent of tyrosine kinase inhibitors (TKIs), which bind to the kinase domain of BCR-ABL fusion protein, leading to the elimination of leukemic cells (3, 4).

Several deubiquitinating enzyme (DUB) genes such as *A20 (Tnfaip3), CYLD* and *Otubain 1* are considered as inflammatory and tumor suppressors by negatively regulating cell proliferation/differentiation and survival through deubiquitinating several key signaling proteins such as NF-κBs and STATs (5-7). A20 is known to inhibit proliferation and induce apoptosis of CML cell lines, CML, and $CD34^+$CML cells via miR-17-92 (8). *A20* expression is down-regulated in lymphoma (6) and chronic lymphocytic leukemia (CLL) (9), whereas other investigations on glioblastoma, hepatocellular carcinoma, and acute lymphoblastic leukemia (ALL) cells reveal its increased expression (10, 11). Similar to A20, CYLD is also indicated as a critical mediator in cell survival in ALL and CLL cells (7, 12). The presence of *OTUB1* is linked to poor migration of colorectal cancer (13) and *OTUB1*-deficient mice exhibit late embryonic lethality (5). Up to now, investigations on the effects of the DUB genes such as *A20, CYLD, Otubain 1, Otubain 2* and *Cezanne* on the function of myeloid leukemic cells have been poorly studied.

Vinblastine (Vinb) and vincristine (Vinc) are Vinca alkaloids derived from the leaves of Catharanthus roseus and extensively used as antimitotic drugs in combination with chemotherapy in a variety of neoplasms, including leukemias and lymphomas (14). The difference between Vinb and Vinc is that Vinb has a methyl group, while Vinc has a formyl group on the indole nitrogen of the vindoline skeleton (15). The small difference between Vinb and Vinc leads to distinct toxicity, although they both exert potential anticancer effects by inhibiting the assembly of tubulin and disrupting microtubule function, which causes

* Corresponding author. Email: xuannt@igr.ac.vn

multinucleated cells and cell death (15, 16). Side-effects of Vinc consist of toxicity to the nervous system. Unlike the toxic effect of Vinc, Vinb toxicity usually involves the hematopoietic system (17) and neurotoxicity is less frequent with Vinb as compared with Vinc (17). The anti-carcinogenic effects of the two products have been shown to be partly mediated through the activation of NF-κB and STAT pathways (18).

Little is known regarding the involvement of the DUB genes in the regulation of proliferation and apoptosis of CML (K562) cells upon challenge with Vinb/Vinc. The present study has thus been performed to elucidate whether the presence of *A20* and *CYLD* contribute to their regulatory effects on the function of CML cells in response to Vinb/Vinc. To this end, the gene expression profile, activation, proliferation and survival of CML cells were investigated.

Materials and Methods

Patients and control subjects

Total peripheral blood samples from untreated 96 BCR/ABL-positive CML patients with newly diagnosed chronic phase and 80 normal healthy volunteers without CML signs, used as controls, were collected at the 103 Hospital, Military Medical University and the National Institute of Hematology and Blood Transfusion, Hanoi, Vietnam. The patients were diagnosed as CML according to the criteria of the World Health Organization (WHO) (19). No individuals in the control population took any medication or suffered from any known acute or chronic disease. All patients and volunteers gave written consent to participate in the study. Person care and experimental procedures were performed according to Vietnamese law for the welfare of human and were approved by the Ethical Committee of the Institute of Genome Research, Vietnam Academy of Science and Technology.

Isolation of CML cells and PBMCs

Peripheral blood mononuclear cells (PBMCs) from CML patients and healthy donors, respectively, were collected by venipuncture and transferred to sterile tubes containing EDTA as an anticoagulant and isolated via density gradient centrifugation (Ficoll-Paque Plus, GE Healthcare Life Sciences). The cells were next counted in a Neubauer chamber, washed with PBS and used for further experiments.

Drugs and culture of K562 cells

BCR/ABL positive CML cell line K562 was purchased from American Type Culture Collection and cultured in RPMI 1640 (GIBCO) containing: 10 % FCS, 1 % penicillin/streptomycin, and 1 % glutamine. Cells were maintained in cell culture dishes at 37°C with a humidified atmosphere containing 5% CO_2. All experiments were performed on the cells at passages 3-8 with 80%-90% confluence. Vincristine and Vinblastine were purchased from Sigma Aldrich and dissolved in DMSO. The drugs were stored at-20°C and protected from light.

Immunostaining and flow cytometry

The surface expressions of CD11b, CD86, CD40, CD3, CD4, CD8, CD19, CD25, CD44 and CD45 were determined by FACS analysis. To this end, cells (10^5) were incubated in 100 µl FACS buffer (phosphate-buffered saline (PBS) plus 0.1% FCS) containing fluorochrome-conjugated antibodies at a concentration of 10 µg/ml. After incubating with the antibodies for 60 min at 4^0C, the cells were washed twice and resuspended in FACS buffer for flow cytometry analysis (FACSAria Fusion, BD Biosciences).

Cytokine quantification

CML cells were transfected with control or *A20* or *CYLD* siRNA for 48 h and then treated with Vinb (Sigma Aldrich) or Vinc (Sigma Aldrich) for another 24 h. Cell culture supernatant was collected and stored at -20˚C until used for ELISA. IL-1β, TNF-α, and IL-6 concentrations were determined by using ELISA kits (Thermo Scientific) according to the manufacturer's protocol.

RNA extraction and real-time RT-PCR

Total mRNA was isolated using the Qiashredder and RNeasy Mini Kit from Qiagen according to the manufacturer's instructions. For cDNA first-strand synthesis, 1 µg of total RNA in 12.5 µl DEPC-H_2O was mixed with 1 µl of oligo-dT primer (Invitrogen) and heated for 2 min at 70°C. To determine transcript levels of *A20, CYLD, Otubain 1, Otubain 2*, *Cezanne, SHP-1, SHP-2, STAT-1, STAT-3, STAT-5, STAT-6* and GAPDH, the quantitative real-time PCR with the LightCycler System (Roche Diagnostics)

Table 1. Primer sequences used for the quantitative PCR experiments.

Gene	Forward (5'→3')	Reverse (5'→3')
A20	TCCTCAGGCTTTGTATTTGA	TGTGTATCGGTGCATGGTTTT
CYLD	TGCCTTCCAACTCTCGTCTTG	AATCCGCTCTTCCCAGTAGG
Otubain 1	ACAGAAGATCAAGGACCTCCA	CAACTCCTTGCTGTCATCCA
Otubain 2	CTCACGTCGGCCTTCATCA	GCCATGGGCTCTACTTCGT
Cezanne	ACAATGTCCGATTGGCCAGT	ACAGTGGGATCCACTTCACATTC
CYLD	TGCCTTCCAACTCTCGTCTTG	AATCCGCTCTTCCCAGTAGG
SHP-1	GCC CAG TTC ATT GAA ACC AC	GAG GGA ACC CTT GCT CTT CT
SHP-2	GAGAGCAATGACGGCAAGTCT	CCTCCACCAACGTCGTATTTC
STAT1	CCCTTCTGGCTTTGGATTGAA	CTTCCCGGGAGCTCTCACTGA
STAT3	GGA GGA GTT GCA GCA AAA AG	TGT GTT TGT GCC CAG AAT GT
STAT5	CAGACCAAGTTTGCAGCCAC	CACAGCACTTTGTCAGGCAC
STAT6	GCCCACTCACTCCAGAGGACCT	GGTGTTGGGGAAAGTCGACAT
GAPDH	GGAGCGAGATCCCTCCAAA	GGCTGTTGTCATACTTCTCAT

was applied. The qPCR primer information in this study is summarized in Table 1. PCR reactions were performed in a final volume of 20 µl containing 2 µl cDNA, 2.4 µl $MgCl_2$ (3 µM), 1 µl primer mix (0.5 µM of both primers), 2 µl cDNA Master SybrGreen I mix (Roche Molecular Biochemicals), and 12.6 µl DEPC-treated water. The target DNA was amplified during 40 cycles of 95ºC for 10 s, 62ºC for 10 s, and 72ºC for 16 s, each with a temperature transition rate of 20ºC/s, a secondary target temperature of 50ºC, and a step size of 0.5ºC. Melting curve analysis was performed at 95ºC, 0 s; 60ºC, 10 s; 95ºC, 0 s to determine the melting temperature of primer dimers and the specific PCR products. The ratio between the respective gene and corresponding GAPDH was calculated per sample according to the ΔΔ cycle threshold method (20).

Transfection of cells with siRNAs

Control- or *A20*- or *CYLD*-targeted siRNA (Thermo Fisher Scientific) was transfected into cells (10^5 cells/1ml) with the help of Lipofectamine RNAiMAX Reagent (Invitrogen) according to the manufacturer's recommendations. After 48h transfection, cells were treated with Vinb or Vinc for another 24 h at 37ºC, 5% CO_2. After washing three times with PBS, cells were used for experiments.

Proliferation assay

The cells were washed twice with PBS and then labeled with a 10-µM solution of 5,6-carboxyfluorescein diacetate succinimidyl ester (CFSE) ($2x10^5$ cells/mL) and incubated at 37ºC/5% CO_2 for 10 minutes. The cells were washed and centrifuged to remove excessive CFSE. CFSE-labeled cells were cultured in 24-well plates ($2x10^5$ cells/ mL) at 37ºC/5% CO_2 for 5 days. The cells were harvested, washed twice and then resuspended in FACS buffer, and the fluorescence was analyzed with flow cytometry.

Phosphatidylserine translocation and propidium iodide incorporation

The presence of phosphatidylserine (PS) on the outer surface of apoptotic cells was detected with fluorescein isothiocyanate (FITC)-conjugated annexin V binding to PS at the cell surface and necrosis was assessed from the amount of propidium iodide (PI)-positive cells. In brief, 10^5 cells were harvested and washed twice with Annexin washing buffer (AWB). The cell pellet was resuspended in 100 µl of Annexin V/PI labelling solution (eBioscience), and incubated for 15 min at room temperature. After washing with AWB, the cells were analyzed by flow cytometry.

Determination of ROS production

ROS production in CML cells was determined utilizing 2′,7′-dichlorodihydrofluorescein diacetate (DCFDA, Sigma). After the treatment, the cells were collected and DCFDA was added to cell suspension at a final concentration of 10 µM. After 30 minutes of incubation in the dark at 37°C, cells were centrifuged and the pellet was washed twice with ice-cold PBS. The pellet was then resuspended in FACS buffer and the fluorescence was analyzed with flow cytometry.

Statistics

Data are provided as means ± SEM, n represents the number of independent experiments. Differences were tested for significance using Student's unpaired two-tailed t-test or ANOVA, as appropriate. $P<0.05$ was considered statistically significant.

Results

Clinical correlations

Clinical features of the CML patient group are listed in Table 1. Results indicated that the percentage of female CML patients was 37%. The median age of CML patients at diagnosis was 46.71 years. Among clinical biomarkers assessed in Table 2, CML patients had all median total protein, Ferritin and LDH levels higher than normal values. Importantly, the percentages of CML patients with Ferritin and LDH levels higher than their clinical cutoff were

Table 2. Clinical characteristics of CML patients.

Characteristics	Patients with higher-than-normal values (n, %)	Mean	Standard deviation (SD)	Normal range
Mean age at diagnosis (range)		46.71 (16-81)		
Female (%)		38.54 (37)		
Urea (mmol/l)	4 (4.17%)	5.18	1.33	7.5
Glucose (mmol/l)	20 (20.83%)	5.99	1.47	6.4
Creatinine (µmol/l)	4 (4.17%)	82.10	20.72	120 (M)/100 (F)
Uric acid (µmol/l)	15 (15.63%)	309.23	92.95	420 (M)/360 (F)
Total bilirubin (µmol/l)	12 (12.5%)	12.03	6.77	17
Direct bilirunbin (µmol/l)	12 (12.5%)	2.69	2.06	4.3
Indirect bilirubin (µmol/l)	13 (13.54%)	9.49	5.21	12.7
Total protein (g/l)	13 (13.54%)	**83.74**	58.03	82
Albumin (g/l)	0 (0%)	41.96	6.74	50
Globulin (g/l)	10 (10.42%)	33.70	7.27	38
Ferritin (µg/l)	47 (48.96%)	**399.55**	382.61	400
AST (U/l)	16 (16.67%)	32.03	28.87	37
ALT (U/l)	17 (17.71%)	35.67	45.96	40
LDH (U/l)	49 (51.04%)	**542.04**	300.89	460

AST: aspartate transaminase; ALT: alanine aminotransferase; LDH: lactate dehydrogenase.

48.96 and 51.04%, respectively.

Analysis of gene expression profile in CML cells

We firstly examined the expression of the DUBs genes and found that mRNA levels of *A20, CYLD, Cezanne* and *Otubain1* were significantly down-regulated in CML cells. However, no difference in transcriptional expression of *Otubain2* gene in the patient and control groups was detected (Figure 1A).

A20, CYLD and *Otubain1* are known to inhibit inflammatory response through several signalling pathways, including SHPs, NF-κBs and STATs (5, 21, 22). Similar to the DUBs, the mRNA level of *SHP-1* was significantly lower, while the expression of *SHP-2* was significantly higher in the CML group compared to controls (Figure 1B). In agreement, several previous studies on patients with multiple myeloma and T-cell leukemia reported an inactivated expression of *SHP-1* (23, 24), which is linked to the activation of the JAK/STAT pathway in these patients. As expected, mRNA levels of *STAT1* and *STAT6*, but not *STAT3* and *STAT5,* were significantly increased in CML cells (Figure 1C).

Immunophenotypic change of CML cells

Next, we investigated changes in activation of myeloid ($CD11b^+$), CD4 T ($CD3^+$ $CD4^+$), CD8 T ($CD3^+$ $CD8^+$) and B ($CD19^+$) cells present in CML by flow cytometry. The $CD45^+$ cells were gated in all experiments. Flow cytometry analysis showed that numbers of $CD11b^+$ $CD86^+$ and $CD3^+CD4^+CD25^+$ expressing cells were significantly accumulated, whereas percentages of $CD11b^+$ $CD40^+$, $CD3^+CD4^+CD44^+$, $CD3^+CD8^+CD44^+$, $CD19^+CD25^+$ and $CD19^+CD44^+$ expressing cells were unaltered in CML patients (Figure 2A-B). In addition, the percentage of $CD3^+CD8^+CD25^+$ cells was higher in CML than that in controls but not reaching to the statistical difference (Figure 2B).

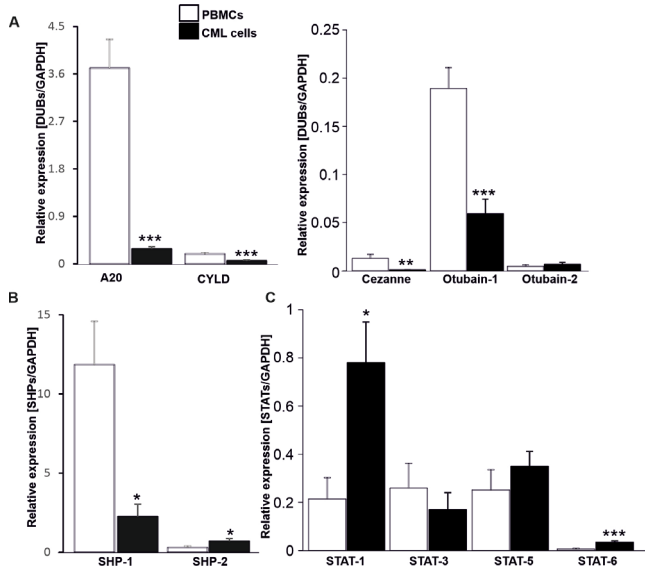

Figure 1. Expression of DUB, STATs and SHPs genes in CML patients. A. Arithmetic means ± SEM (n = 7 each) of transcript levels of *A20, CYLD, Cezanne, Otubain1* and *Otubain*2, which are shown to control (white bars) and CML cells (black bars). GAPDH was used as a reference gene for relative quantification. ** ($p<0.01$) and *** ($p<0.001$) indicate significant differences from control PBMCs (ANOVA). **B.** Arithmetic means ± SEM (n = 7 each) of transcript levels of *SHP1, SHP2, STAT1, STAT3, STAT5* and *STAT6*, which are shown to control (white bars) and CML cells (black bars). GAPDH was used as a reference gene for relative quantification. * ($p<0.05$) and *** ($p<0.001$) indicate significant differences from control PBMCs (ANOVA).

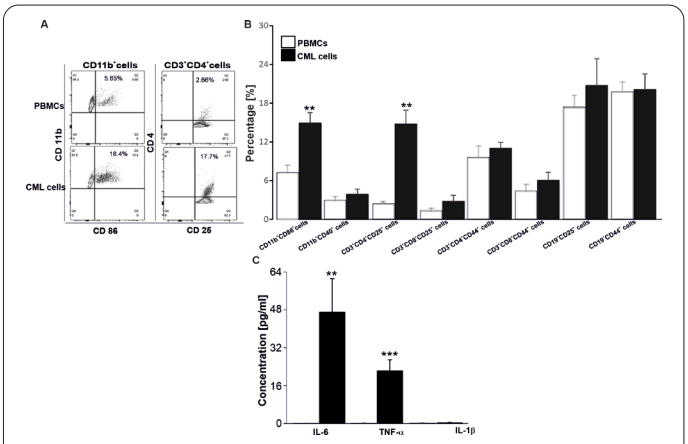

Figure 2. Immunophenotypic feature in CML patients. A. Original dot plots of $CD11b^+CD86^+$ and $CD3^+$ $CD4^+$ $CD25^+$ expressing cells, which are shown to control PBMCs (upper panels) and CML cells (lower panels). All samples were gated with $CD45^+$ live cells. **B.** Arithmetic means ± SEM (n = 7 each) of percentages of $CD11b^+CD86^+$, $CD11b^+CD40^+$, $CD3^+$ $CD4^+$ $CD25^{++}$, $CD3^+$ $CD8^+$ $CD25^{+}$ $^{+}$, $CD3^+$ $CD4^+$ $CD44^+$, $CD3^+$ $CD8^+$ $CD44^+$, $CD19^+$ $CD25^+$ and $CD19^+$ $CD44^+$ expressing cells, which are shown to control (white bars) and CML cells (black bars). ** ($p<0.01$) indicates significant difference from control PBMCs (ANOVA). **C.** Arithmetic means ± SEM (n = 80-96 each) of IL-6, TNF-α, and IL-1β concentrations, which are attained from sera of healthy donors (white bars) and CML patients (black bars). ** ($p<0.01$) and *** ($p<0.001$) indicate significant differences from healthy donors (ANOVA).

For cytokine analysis of sera, levels of IL-6, TNF-α, and IL-1β were measured by ELISA. Results showed that IL-6 and TNF-α concentrations in CML patients were found to be higher than in control individuals. However, CML patients showed no change in the serum level of IL-1β (Figure 2C). The evidences indicated that inactivated expression of *A20, CYLD, Cezanne* and *Otubain1* in CML cells could be involved in the activation of $CD11b^+$ and CD4 T cells and secretion of IL-6 and TNF-α in the circulatory system.

Effects of Vinb and Vinc on proliferation and survival of K562 cells

Vinb and Vinc are known to induce apoptosis of lymphocytic leukemia and lymphoma cells (25, 26); therefore, we conducted experiments to ask whether the influence of Vinb (20-120nM) or Vinc (60-300nM) on the function of CML (K562) cells. As shown in Figure 3A, treatment of K562 cells with Vinb (120nM)/Vinc (300nM) significantly reduced the percentage of CFSE-positive cells as well as significantly enhanced the number of Annexin V^+PI^- cells and accumulation of ROS. The release of IL-6 and TNF-α in these cells was slightly increased upon treatment with Vinb/Vinc, but not reaching statistical differences (Figure 3B). In addition, we examined the expression of CD86 on $CD11b^+$ cells and of CD25 on CD4T cells as well as levels of SHPs and STATs genes and observed that no difference in these markers was found in control and Vinb/Vinc-treated cells (data not shown). The evidences suggested that Vinb (120nM)/Vinc (300nM) affected the proliferation

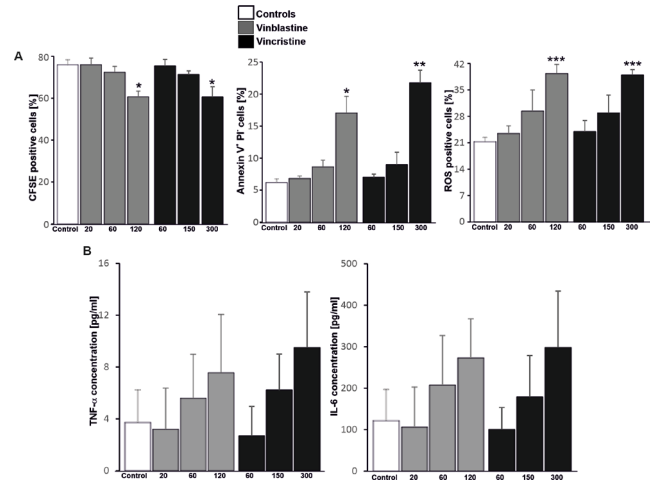

Figure 3. Effect of Vinb/Vinc on the function of K562 cells. A. Arithmetic means ± SEM (n = 5 each) of $CFSE^+$, Annexin V^+PI^- and ROS^+ cells, which were either untreated (white bars) or treated with Vinb (20, 60 and 120 nM, grey bars) or Vinc (60, 150 and 300 nM, black bars). * (p<0.05), ** (p<0.01) and *** (p<0.001) indicate significant differences from controls (ANOVA). **B.** Arithmetic means ± SEM (n = 5 each) of IL-6 and TNF-α concentrations are attained from supernatants of K562 cells, which were either untreated (white bars) or treated with Vinb (20, 60 and 120 nM, grey bars) or Vinc (60, 150 and 300 nM, black bars).

and survival of K562 cells rather than their activation and maturation.

Effect of A20 and CYLD on the proliferation of Vinc-treated K562 cells

Since expression of *A20, CYLD, Cezanne* and *Otubain1* was downregulated in CML cells. Hence, we examined levels of the DUB genes when K562 cells were exposed to Vinb (20-120nM) or Vinc (60-300nM). Results indicated that mRNA levels of *A20* and *CYLD,* but not *Cezanne* and *Otubain1* were significantly higher when the cells were treated with Vinc at a concentration of 300nM (Figure 4A). In addition, the expression of the other DUBs was unaltered in the presence of Vinb (data not shown).

To ask whether the changes in the function of K562 cells are related to the expression of *A20* and *CYLD*. The cells were transfected with control or *A20* or *CYLD* siRNA and followed by Vinc (300nM) treatment. The efficiency of transcriptional expression was tested by real-time PCR, and results showed that *A20/CYLD* siRNA effectively decreased the expression of *A20/CYLD* in PBMCs (Figure 4B).

To examine whether the proliferation of K562 cells when exposed with Vinc (300nM) is related to expression of *A20* and *CYLD*, the cells were stained with CFSE and cultured for 5 days. As shown in Figure 4C-D, the proliferation activity of K562 cells was markedly reduced when treated with Vinc. The effect was abolished in the presence of *A20* or *CYLD* siRNA, pointing out that the inhibitory effect of Vinc on cell proliferation was sensitive to the presence of *A20* and *CYLD.*

Effect of A20 on Vinc-treated K562 cell death

To examine whether the diminished proliferation rate of K562 cells is related to cell death, experiments using Annexin V/PI and DCFDA stainings were conducted in these cells. As seen in Figure 5A-D, treatment of Vinc (300nM) significantly enhanced the number of Annexin V^+PI^- cells

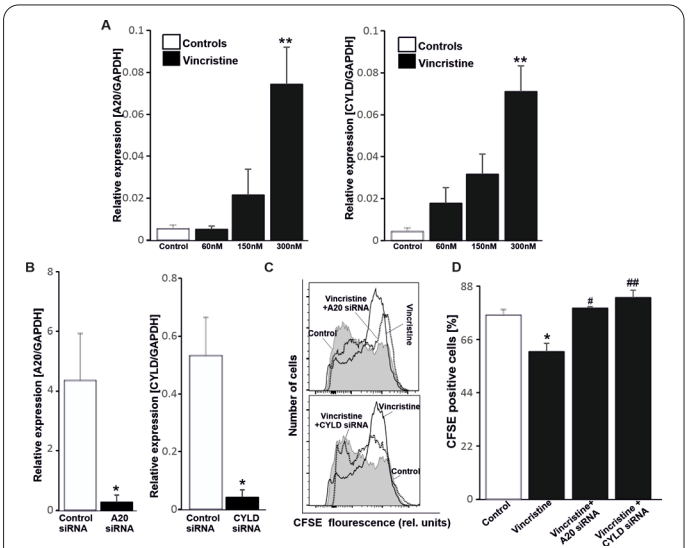

Figure 4. Effect of A20 and CYLD on the proliferation of K562 cells. A. Arithmetic means ± SEM (*n* = 5 each) of transcript levels of *A20* and *CYLD* in K562 cells, which were either untreated (white bars) or Vinc (60, 150 and 300 nM, black bars). ** (p<0.01) indicates a significant difference from controls (ANOVA). **B**. Arithmetic means ± SEM (*n* = 5 each) of transcript levels of *A20* and *CYLD* in PBMCs, which were transfected with control siRNA (white bars) or A20 siRNA/CYLD siRNA (40nM, black bars). GAPDH was used as a reference gene for relative quantification. * (p<0.05) indicates a significant difference from controls (ANOVA). **C.** Representative FACS histograms depicting CFSE fluorescence are attained from K562 cells, which were untreated or treated with Vinc (300 nM) in the presence or absence of A20 siRNA/CYLD siRNA (40nM). **D.** Arithmetic means ± SEM (*n* = 5 each) of CFSE positive cells, which were untreated (white bar) or treated with Vinc (black bars, 300 nM) in the presence or absence of A20 siRNA/CYLD siRNA (40nM). * (p<0.05) indicates significant difference from controls; # (p<0.05) and ## (p<0.01) indicate significant differences from Vinc-treated K562 cells (ANOVA).

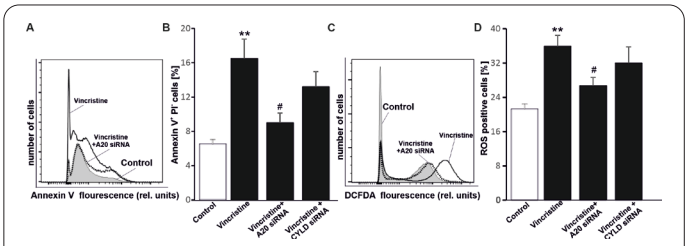

Figure 5. Effect of A20 and CYLD on survival of K562 cells. A, C. Representative FACS histograms depicting Annexin V (**A**) and DCFDA (**C**) fluorescences were attained from K562 cells, which were untreated or treated with Vinc (300 nM) in the presence or absence of A20 siRNA (40nM). **B, D.** Arithmetic means ± SEM (*n* = 5 each) of Annexin V^+PI^- (**B**) and ROS^+ (**D**) cells, which were untreated (white bar) or treated with Vinc (black bars, 300 nM) in the presence or absence of A20 siRNA (40nM). ** (p<0.01) indicates significant difference from controls; # (p<0.05) indicates significant difference from Vinc-treated K562 cells (ANOVA).

and accumulation of ROS. The effects were attenuated in the presence of *A20* siRNA, but not *CYLD* siRNA.

Discussion

Inactivated expression of *A20, CYLD, Cezanne* and *Otubain1* genes in CML patients was revealed for the first time. Recently, inactivation of *A20* has been found in patients with acute lymphocytic leukemia (ALL) (27),

Cezanne downregulation is linked to poor prognosis in hepatocellular carcinoma (28) and aberrant expression in *CYLD* gene is reported in leukemia and lymphoma (29, 30). *A20, CYLD* and *Otubain1* are considered as negative regulators of immune reaction through NF-κBs and/or STATs pathways (5, 21, 22), whose constitutive activation is related to the development of hematologic malignancy (2). As expected, we observed that the expression of *STAT1* and *STAT6* was significantly enhanced in CML patients as compared to controls. Activated *STAT6* has been found in patients with solid cancers, lymphoma and leukemia and is involved in cellular proliferation and transformation (31). Moreover, we indicated that the level of *SHP-1* was lower, while *SHP-2* expression was higher in CML patients compared to controls. Consistently, several studies reported the inactivated expression of *SHP-1* in hematological malignancies (23, 32) and SHP-2 phosphorylation is associated with imatinib-resistance phenotype in CML patients (33).

The immunophenotypic profile of CML cells indicated that $CD11b^+CD86^+$ and $CD3^+CD4^+CD25^+$ expressing cells were recruited into the circulatory system. Recent studies show that level of CD86 is highly expressed in leukemia (34) and associated with T-cell exhaustion and relapse risk (35). The account of CD86-positive plasmacytoid dendritic cells is higher in CML cells than in normal PBMCs (35). Differently, the expression of CD40 has diverse effects on cell function. It is linked to inducing an immune response (36) and increasing malignant cell growth, survival, and immunogenicity (37). The level of CD25 is also indicated to express at a higher level on CML stem cells (38) and is associated with poor prognosis in CML (39). Gene expression is a process in which the information contained in the gene is used to obtain a functional product from it (40-42).

The promoting roles of Vinb and Vinc on cell death in lymphocytic leukemia and lymphoma are shown in several studies (25, 26). In this study, we observed the inhibitory effects of Vinb and Vinc on the proliferation and survival of K562 cells, as the reduced expression of CFSE-positive cells and the increased number of Annexin V^+PI^- cells and ROS accumulation were detected in the presence of Vinb (120nM) or Vinc (300nM). Vinb and Vinc are known to exert inhibitory effects on cell proliferation by binding to the microtubules to prevent the development of the mitotic spindle (43). In addition, we showed that Vinb/Vinc did not affect the activation and maturation of K562 cells.

Importantly, the mRNA levels of *A20* and *CYLD* were significantly enhanced in K562 cells and slightly increased in PBMCs (data not shown) when treated with Vinc. Therefore, the cells were silenced by using *A20* or *CYLD* siRNA. As expected, the inhibitory effects on proliferation and survival of K562 cells were abolished by the presence of *A20* siRNA and the cell proliferation only was sensitive to *CYLD* expression upon challenge with Vinc. This finding is supported by other reports indicating that the promoting effect of *A20* on cell death has been investigated in several cell types, including lymphoma (6), CLL (9), and myeloid leukemic cells (8), whereas *A20* is considered as a negative regulator of cell apoptosis in glioblastoma, hepatocellular carcinoma, and ALL (10, 11). Besides, A20 is also known to suppress cell proliferation and metastasis (8). In comparison with *A20*, the role of *CYLD* was a less potent effector in modulating the apoptosis of K562 cells. Up to now, there has been no report about the regulatory role of *CYLD* on the function of myeloid leukemic cells, although *CYLD* is reported as a positive regulator of cell apoptosis in ALL and CLL cells (7, 12). In addition, mRNA levels of *A20* and *CYLD* were unaffected upon treatment of K562 cells with Vinb (data not shown). Clearly, Vinb and Vinc differ in their regulation of cellular biological activities. Vinc has the potential to induce neurotoxicity, while hematologic toxicity is rarely related to Vinc (17).

In conclusion, the present study discloses that Vinc inhibits cell proliferation and survival of K562 cells through upregulated *A20* expression. The events might contribute to the anticancer effect of Vinc on *A20*-sensitive CML cells.

Competing interests

The authors of this paper declare that they have no financial/commercial conflicts of interest.

Acknowledgment

This research is funded by the Vietnam Academy of Science and Technology (VAST) under grant number VNNS. VAST.02.

References

1. Druker BJ, Guilhot F, O'Brien SG, Gathmann I, Kantarjian H, Gattermann N, et al. Five-year follow-up of patients receiving imatinib for chronic myeloid leukemia. N Engl J Med. 2006; 355(23):2408-17.
2. He Q, Dong J, Zhen H, Ying Y, Zhang J, Li Q, et al. A small molecule significantly inhibits the bcr/abl fusion gene at the mRNA level in human chronic myelogenous leukemia. Leuk Res. 2011; 35(8):1074-9.
3. Becker C, Fantini MC, Schramm C, Lehr HA, Wirtz S, Nikolaev A, et al. TGF-beta suppresses tumor progression in colon cancer by inhibition of IL-6 trans-signaling. Immunity. 2004; 21(4):491-501.
4. Tebbutt NC, Giraud AS, Inglese M, Jenkins B, Waring P, Clay FJ, et al. Reciprocal regulation of gastrointestinal homeostasis by SHP2 and STAT-mediated trefoil gene activation in gp130 mutant mice. Nat Med. 2002; 8(10):1089-97.
5. Mulas F, Wang X, Song S, Nishanth G, Yi W, Brunn A, et al. The deubiquitinase OTUB1 augments NF-kappaB-dependent immune responses in dendritic cells in infection and inflammation by stabilizing UBC13. Cell Mol Immunol. 2021;18(6):1512-1527
6. Wang X, Xu Y, Liang L, Xu Y, Wang C, Wang L, et al. Abnormal expression of A20 and its regulated genes in peripheral blood from patients with lymphomas. Cancer Cell Int. 2014; 14(36).
7. Xu X, Kalac M, Markson M, Chan M, Brody JD, Bhagat G, et al. Reversal of CYLD phosphorylation as a novel therapeutic approach for adult T-cell leukemia/lymphoma (ATLL). Cell Death Dis. 2020; 11(2):94.
8. Jia Q, Sun H, Xiao F, Sai Y, Li Q, Zhang X, et al. miR-17-92 promotes leukemogenesis in chronic myeloid leukemia via targeting A20 and activation of NF-kappaB signaling. Biochem Biophys Res Commun. 2017; 487(4):868-74.
9. Frenzel LP, Claus R, Plume N, Schwamb J, Konermann C, Pallasch CP, et al. Sustained NF-kappaB activity in chronic lymphocytic leukemia is independent of genetic and epigenetic alterations in the TNFAIP3 (A20) locus. Int J Cancer. 2011; 128(10):2495-500.
10. Chen S, Xing H, Li S, Yu J, Li H, Liu S, et al. Up-regulated A20 promotes proliferation, regulates cell cycle progression and induces

chemotherapy resistance of acute lymphoblastic leukemia cells. Leuk Res. 2015; 39(9):976-83.
11. Hjelmeland AB, Wu Q, Wickman S, Eyler C, Heddleston J, Shi Q, et al. Targeting A20 decreases glioma stem cell survival and tumor growth. PLoS Biol. 2010; 8(2):e1000319.
12. Liu P, Xu B, Shen W, Zhu H, Wu W, Fu Y, et al. Dysregulation of TNFalpha-induced necroptotic signaling in chronic lymphocytic leukemia: suppression of CYLD gene by LEF1. Leukemia. 2012; 26(6):1293-300.
13. Zhou Y, Wu J, Fu X, Du W, Zhou L, Meng X, et al. OTUB1 promotes metastasis and serves as a marker of poor prognosis in colorectal cancer. Mol Cancer. 2014; 13(258).
14. Owellen RJ, Hartke CA, Dickerson RM, Hains FO. Inhibition of tubulin-microtubule polymerization by drugs of the Vinca alkaloid class. Cancer Res. 1976; 36(4):1499-502.
15. Jordan MA, Himes RH, Wilson L. Comparison of the effects of vinblastine, vincristine, vindesine, and vinepidine on microtubule dynamics and cell proliferation in vitro. Cancer Res. 1985; 45(6):2741-7.
16. Howard SM, Theologides A, Sheppard JR. Comparative effects of vindesine, vinblastine, and vincristine on mitotic arrest and hormonal response of L1210 leukemia cells. Cancer Res. 1980; 40(8 Pt 1):2695-700.
17. Moudi M, Go R, Yien CY, Nazre M. Vinca alkaloids. Int J Prev Med. 2013; 4(11):1231-5.
18. Shakeri A, Gahnbari M, Tasbandi A, Sahebkar A. Regulation of microRNA-21 expression by natural products in cancer. Phytother Res. 2021; 35(7):3732-3746.
19. Arber DA, Orazi A, Hasserjian R, Thiele J, Borowitz MJ, Le Beau MM, et al. The 2016 revision to the World Health Organization classification of myeloid neoplasms and acute leukemia. Blood. 2016; 127(20):2391-405.
20. Livak KJ, Schmittgen TD. Analysis of relative gene expression data using real-time quantitative PCR and the 2(-Delta Delta C(T)) Method. Methods. 2001; 25(4):402-8.
21. Wang X, Deckert M, Xuan NT, Nishanth G, Just S, Waisman A, et al. Astrocytic A20 ameliorates experimental autoimmune encephalomyelitis by inhibiting NF-kappaB- and STAT1-dependent chemokine production in astrocytes. Acta Neuropathol. 2013; 126(5):711-24.
22. Nishanth G, Deckert M, Wex K, Massoumi R, Schweitzer K, Naumann M, et al. CYLD enhances severe listeriosis by impairing IL-6/STAT3-dependent fibrin production. PLoS Pathog. 2013; 9(6):e1003455.
23. Chim CS, Fung TK, Cheung WC, Liang R, Kwong YL. SOCS1 and SHP1 hypermethylation in multiple myeloma: implications for epigenetic activation of the Jak/STAT pathway. Blood. 2004; 103(12):4630-5.
24. Zhang Q, Wang HY, Marzec M, Raghunath PN, Nagasawa T, Wasik MA. STAT3- and DNA methyltransferase 1-mediated epigenetic silencing of SHP-1 tyrosine phosphatase tumor suppressor gene in malignant T lymphocytes. Proc Natl Acad Sci U S A. 2005; 102(19):6948-53.
25. Bates DJ, Danilov AV, Lowrey CH, Eastman A. Vinblastine rapidly induces NOXA and acutely sensitizes primary chronic lymphocytic leukemia cells to ABT-737. Mol Cancer Ther. 2013; 12(8):1504-14.
26. Toh HC, Sun L, Koh CH, Aw SE. Vinorelbine induces apoptosis and caspase-3 (CPP32) expression in leukemia and lymphoma cells: a comparison with vincristine. Leuk Lymphoma. 1998; 31(1-2):195-208.
27. Canh NX, Giang NV, Nghia VX, Sopjani M, Ngan NTT, Hoang NH, et al. Regulation of cell activation by A20 through STAT signaling in acute lymphoblastic leukemia. J Recept Signal Transduct Res. 2021; 41(4):331-8.
28. Wang JH, Wei W, Guo ZX, Shi M, Guo RP. Decreased Cezanne expression is associated with the progression and poor prognosis in hepatocellular carcinoma. J Transl Med. 2015; 13(41.
29. Arora M, Kaul D, Varma N. Functional nature of a novel mutant CYLD observed in pediatric lymphoblastic B-cell leukemia. Pediatr Blood Cancer. 2015; 62(6):1066-9.
30. Wu W, Zhu H, Fu Y, Shen W, Xu J, Miao K, et al. Clinical significance of down-regulated cylindromatosis gene in chronic lymphocytic leukemia. Leuk Lymphoma. 2014; 55(3):588-94.
31. Bruns HA, Kaplan MH. The role of constitutively active Stat6 in leukemia and lymphoma. Crit Rev Oncol Hematol. 2006; 57(3):245-53.
32. Oka T, Ouchida M, Koyama M, Ogama Y, Takada S, Nakatani Y, et al. Gene silencing of the tyrosine phosphatase SHP1 gene by aberrant methylation in leukemias/lymphomas. Cancer Res. 2002; 62(22):6390-4.
33. Li X, Pang J, Xue W, Wang Y, Tian T, Elgehama A, et al. Inducible SHP-2 activation confers resistance to imatinib in drug-tolerant chronic myeloid leukemia cells. Toxicol Appl Pharmacol. 2018; 360:249-56.
34. Hock BD, Patton WN, Budhia S, Mannari D, Roberts P, McKenzie JL. Human plasma contains a soluble form of CD86 which is present at elevated levels in some leukaemia patients. Leukemia. 2002; 16(5):865-73.
35. Schutz C, Inselmann S, Saussele S, Dietz CT, Mu Ller MC, Eigendorff E, et al. Expression of the CTLA-4 ligand CD86 on plasmacytoid dendritic cells (pDC) predicts risk of disease recurrence after treatment discontinuation in CML. Leukemia. 2017; 31(4):829-36.
36. Xuan NT, Wang X, Nishanth G, Waisman A, Borucki K, Isermann B, et al. A20 expression in dendritic cells protects mice from LPS-induced mortality. Eur J Immunol. 2015; 45(3):818-28
37. Hock BD, McKenzie JL, Patton NW, Drayson M, Taylor K, Wakeman C, et al. Circulating levels and clinical significance of soluble CD40 in patients with hematologic malignancies. Cancer. 2006; 106(10):2148-57.
38. Herrmann H, Sadovnik I, Eisenwort G, Rulicke T, Blatt K, Herndlhofer S, et al. Delineation of target expression profiles in CD34+/CD38- and CD34+/CD38+ stem and progenitor cells in AML and CML. Blood Adv. 2020; 4(20):5118-32.
39. Blatt K, Menzl I, Eisenwort G, Cerny-Reiterer S, Herrmann H, Herndlhofer S, et al. Phenotyping and Target Expression Profiling of CD34(+)/CD38(-) and CD34(+)/CD38(+) Stem- and Progenitor cells in Acute Lymphoblastic Leukemia. Neoplasia. 2018; 20(6):632-42.
40. Ghaheri M, Miraghaee S, Babaei A, Mohammadi B, Kahrizi D, Haghighi ZM, Bahrami G. Effect of Stevia rebaudiana Bertoni extract on sexual dysfunction in Streptozotocin-induced diabetic male rats. Cell Mol Biol 2018;64(2):6-10.
41. Esmaeili F, Ghaheri M, Kahrizi D, Mansouri M, Safavi SM, Ghorbani T, Muhammadi S, Rahmanian E, Vaziri S. Effects of various glutamine concentrations on gene expression and steviol glycosides accumulation in Stevia rebaudiana Bertoni. Cell Mol Biol 2018;64(2):1-5.
42. Ghaheri M, Adibrad E, Safavi SM, Kahrizi D, Soroush A, Muhammadi S, Ghorbani T, Sabzevari A, Ansarypour Z, Rahmanian E. Effects of life cycle and leaves location on gene expression and glycoside biosynthesis pathway in Stevia rebaudiana Bertoni. Cell Mol Biol 2018;64(2):17-22.
43. Keglevich P, Hazai L, Kalaus G, Szantay C. Modifications on the basic skeletons of vinblastine and vincristine. Molecules. 2012; 17(5):5893-914.